VERSITA

OPTO-ELECTRONICS REVIEW **20**(1), 0–0

DOI: 10.2478/s11772-012-0002-5

Liquid crystal alignment in cylindrical microcapillaries

M. CHYCHŁOWSKI*[1], O. YAROSHCHUK[2], R. KRAVCHUK[2], and T. WOLIŃSKI[1]

[1]Faculty of Physics, Warsaw University of Technology, 75 Koszykowa Str., 00-662, Warsaw, Poland
[2]Institute of Physics, NASU, 46 Nauki Ave., 03-028 Kyiv, Ukraine

A variety of alignment configurations of liquid crystals (LCs) inside the glassy cylindrical capillaries is realized by using alignment materials providing different anchoring. The radial configuration with central disclination line is obtained for homeotropic boundary conditions. In turn, the axial, transversal and tilted alignment structures are realized by using materials for planar anchoring. The uniformity and controlling of the latter structures were provided by photoalignment method. This approach can be further used to control LC alignment in the photonic crystal fibers recognized as advanced elements for different optical devices.

Keywords: photonic liquid crystal fibers, photoalignment method, liquid crystal.

1. Introduction

Photonic crystal fibers (PCF) form a new class of optical fibers based on the properties of photonic crystals. The cladding of such fibers is a two-dimensional photonic structure made of rods with diameter of few microns and refractive index different from that in the core. Mostly, these rods are cylindrical tubes filled with air. PCFs have attracted considerable interest in the last decade, because of great potential for various optical applications, such as telecommunication devices, fiber lasers, nonlinear optics, highly sensitive gas sensors, and others [1–4].

The latest developments in the area of PCFs are photonic liquid crystal fibers (PLCFs) [5–9]. In these fibers, cylindrical tubes are filled with a liquid crystal (LC). Comparing with the conventional PCFs, the PLCFs demonstrate greatly improved control of optical properties of cladding. Thermal, electrical, and optical controlling can be realized by influencing LC alignment. The PLCF have potential applications in various optical devices, such as tunable attenuators and filters, polarizers, PMD compensators, and others [10–12].

The light propagation mechanism inside the PLCFs and their tuning range essentially depend on the orientational configuration of LC within the cladding air holes and the photonic structure itself. In the conventional cells, LC is commonly aligned by a direct treatment of the boundary substrates limiting the LC layers. Usually, this alignment treatment can be produced before assembling the cells so that various alignment methods are applicable for this purpose. Depending on properties of the alignment materials and treatment conditions, three basic types of LC alignment can be obtained: homeotropic (perpendicular to the aligning surface), planar (parallel to the surface) and pre-tilted (at some angle to the surface).

LC alignment in the PCF tubes has some peculiarities. Firstly, LC trapped in narrow tubes is strongly and elastically deformed. Thus, together with anchoring, elastic forces, depending on shape and size of the tubes as well as LC orientational elasticity, strongly influence resultant alignment configuration. Secondly, the inner surface of these tubes is not accessible for mechanical (rubbing, molding, etc.) and particle beam alignment treatments [13]. The photoalignment is seemed to be the unique method for this case, since the light is capable to reach the tubes passing through the glassy body of the PCF [14–19]. First attempts in this direction have been recently made [20–24].

The presented paper considers various alignment configurations of LCs in the cylindric tubes with planar and homeotropic boundary conditions. In the tubes with planar anchoring, LC alignment is generated and manipulated with photoalignment technique. The realized alignment structures are studied by means of polarizing microscopy involving host-guest effect in LC systems. Influence of the anchoring and light exposure conditions on LC structures in the capillaries are analyzed.

2. Experimental

2.1. Samples

2.1.1. Model of a PCF tube

To model cylindrical tubes of PCFs and to simplify samples, we have used cylindrical capillaries of 8–25 μm in diameter made of quartz. External diameter of these capillaries was about 90 μm and the length was 8–10 cm. The capillaries were manufactured at the Maria Curie-Skłodowska University (Lublin, Poland).

*e-mail: opto@if.pw.edu.pl

2.1.2. Filling procedure

To fill/extract the alignment material solution or LC into/from the capillary, simple vacuum appliance was used. The capillaries were forcedly filled by creating difference of pressure on their ends. At that, one capillary end was put in the vessel with the filling liquid, while the other was subjected to vacuum of about 400 Pa. For evacuation of filling liquid, one end of the capillary was kept in atmosphere, while the other one was subjected to pressure of 2–3 atmospheres. The infiltration/evacuation time was 5–20 min depending on diameter of the capillary and filling liquid. The filling and evacuation process were controlled by observation samples in polarizing optical microscope.

2.1.3. Alignment coatings

The internal capillary surface was coated by the appropriate aligning material. The homeotropic anchoring has been realized by using n-octadecyltriethoxysilane (Aldrich). As basic photoaligning material for planar alignment we used polyvinylcinnamate (Aldrich) [16–18] and cellulose 4-pentryloxycinnamate (CPC) [25] synthesized at the Institute of Bioorganic and Petrol Chemistry of NASU (Kyiv, Ukraine). Additionally, we used selected diazodyes [26] and bis-methacryllic polymers [27]. In the conventional, sandwich type cells, all these materials provided good LC alignment in the direction perpendicular to the polarization direction of actinic light.

The aligning materials were dissolved in dimethylformamide at concentration of 1 wt.%. The filtered to 0.2-μm solution was filled in the capillary and then the excess part of it was removed from the capillary by using vacuum technique described above. The material remained on the inner capillary wall formed aligning layer after solvent evaporation. To ensure complete removal of solvent and strengthening of aligning layers, the samples were baked at 120°C over 30 min.

In case of planar anchoring, to set alignment direction, the capillaries were exposed to polarized light from the high pressure mercury lamp. The exposure scheme is shown in Fig. 1. Three different exposure geometries were used, with the angle φ between the UV light polarization and the capillary axis equal to 0°, 45°, and 90°, respectively. Usually, the samples were irradiated through a mask to have unexposed and differently exposed sections in the same sample. The exposure time was about 15 minutes.

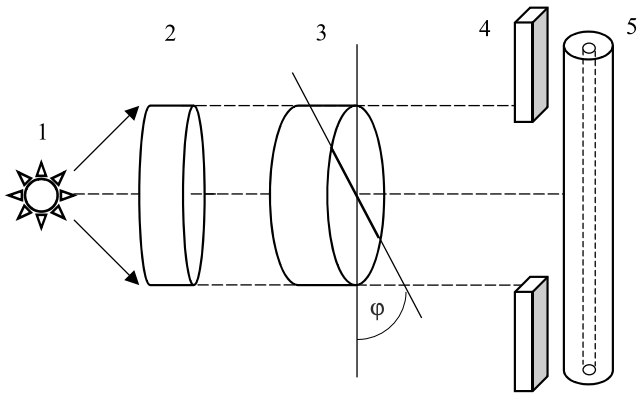

Fig. 1. UV irradiation setup: UV lamp (1), collecting quartz lens (2), UV polarizer (3), mask (4), capillary (5).

2.1.4. LC materials

The capillaries were filled with two nematic LCs' 4-(trans-4'-n-hexylcyclohexyl)-isothiocyanatobenzene (6CHBT) and E7. For additional features in investigation of LC configurations we also used E7 doped with Dispersed Red 1 (DR1) azodye (0.5 wt.%). Molecules of this dichroic dye are isomorphic to molecules of calamitic LCs and so well integrate into their orientational order. This demonstrates Fig. 2, there is obvious that the light polarized along direction of LC alignment is absorbed with the dissolved dye considerably better than the light polarized in the perpendicular direction. Due to this property DR1 is commonly used as a marker detecting direction of LC alignment [28,29].

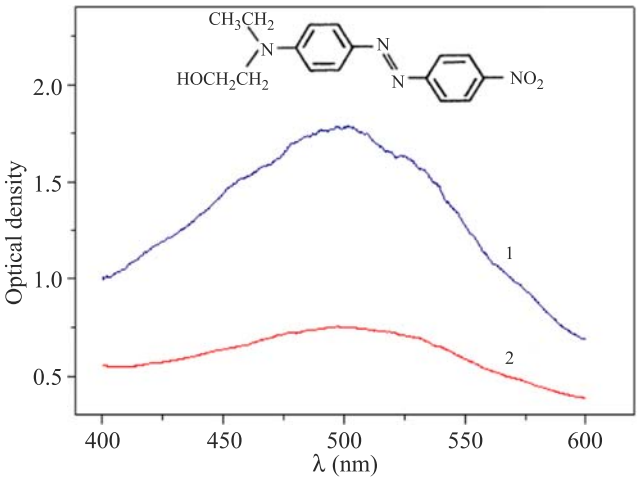

Fig. 2. Polarization spectra of sandwich type LC cell ($d = 15$ μm) for parallel alignment filled with LC E7 doped with the dye DR1 (0.5 wt.%). Spectra 1 and 2 correspond to the light polarization direction parallel and perpendicular to the direction of LC alignment. Since LC E7 does not absorb light in the selected spectral range, the measured spectra reflect absorption of the dichroic dye DR1. Inset shows chemical structure of the dye.

2.2. Methods

LC alignment structures in the capillaries have been identified by observing the samples in polarizing optical microscope. The samples filled with pure LC were viewed between crossed polarizers rotating samples around the axis of optical system and the capillary axis marked in Fig. 3 by the angles α and ϕ, respectively (below, α- and ϕ-rotations). The angle α is set 0° at capillary orientation parallel to the polarizer axis. In turn, the condition $\phi = 0°$ is assigned to the capillary position corresponding to minimization of light transmittance, if this minimization is observable. However, as we noticed, this experiment not always gives enough data for structure identification. Therefore, additionally, the sam-

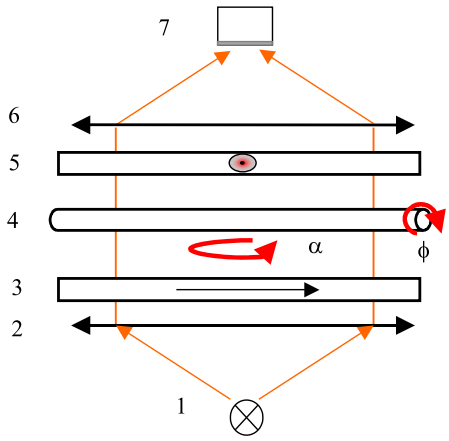

Fig. 3. Scheme demonstrating sample rotation directions during inspection in polarizing microscope: light source (1), condenser (2), polarizer (3), sample (4), analyzer (5), objective (6), camera (7).

ples filled by dyed LC have been investigated. They were observed in polarizing microscope in two regimes with analyzer introduced and removed. In the regime with removed polarizer, we searched positions (directions) corresponding to maximal and minimal sample transmission. Because of parallel alignment of LC and dye molecules, these directions correspond to the direction of LC alignment and the direction perpendicular to LC alignment.

3. Results and discussion

3.1. Alignment configurations in capillaries with planar anchoring

In this section we consider alignment configurations realized in capillaries with planar anchoring provided by photoaligning materials. Because the quality of LC alignment was similar for all these materials and the realized structures depended on geometry of irradiation rather than the material type, we do not specify what material was used in each specific case. The section is divided in three subsections according to three geometries of irradiation with the angle φ between the UV light polarization and the capillary axis equal to 0°, 45°, and 90°, respectively.

3.1.1. Planar alignment

Typical microphotographs corresponding to the angle φ = 90° (Fig. 1) are presented in Fig. 4. By consideration of these samples between crossed polarizers we found out that they become uniformly dark at $\alpha = 0°$ and $\alpha = 90°$ and uniformly bright at $\alpha = 45°$ irrespective of value of the angle ϕ [Fig. 4(a)]. This behaviour allows one to assume that the axis of the induced alignment is parallel to the capillary axis (planar alignment). This conclusion is supported by the behaviour of dyed samples in polarized light demonstrating dark and bright state at orientation parallel and perpendicular to polarizer axis, respectively. The axial alignment configuration is schematically presented in Fig. 5(a).

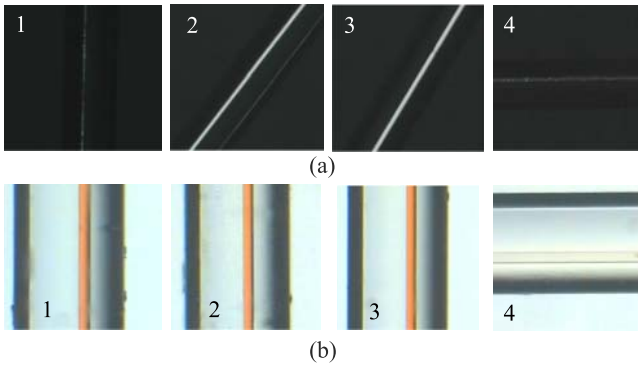

Fig. 4. Microphotographs of the capillary samples with axial LC alignment configuration [Fig. 5(a)]: (a) sample filled with LC 6CHBT viewed between two of crossed polarizers having, accordingly, vertical and horizontal polarization axis: $\alpha = 0°$ (1), $\alpha = 45°$, $\phi = \phi_0$ (2), $\alpha = 45°$, $\phi = \phi_0 + 90°$ (3), $\alpha = 90°$ (4); (b) sample filled with a LC E7 doped with the dichroic DR1 dye viewed in a vertically polarized light: $\alpha = 0°$, $\phi = \phi_0$ (1); $\alpha = 0°$, $\phi = \phi_0 + 45°$ (2); $\alpha = 0°$, $\phi = \phi_0 + 90°$ (3); $\alpha = 90°$, $\phi = \phi_0$ (4).

It is worthwhile mentioning here that the axial alignment configuration has also been observed in the samples not treated by UV light. It is seemingly formed due to a flow alignment effect. However, these samples commonly have multi-domain structure, i.e., poor alignment quality.

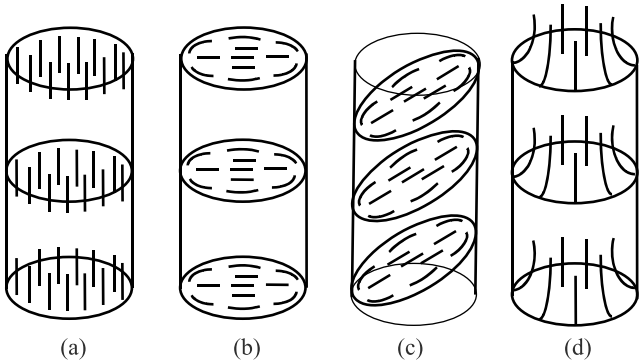

Fig. 5. LC alignment configurations realized in cylindrical microcapillaries with (a–c) planar and (d) homeotropic anchoring conditions: (a) axial configuration, (b) transversal configuration, (c) tilted configuration, (d) escaped radial configuration.

3.1.2. Transversal alignment

The pictures corresponding to polarization angle of UV light $\varphi = 0°$ (Fig. 1) are presented in Fig. 6. In crossed polarizers, at rotation around the axis of optical system, these samples frequently behave similarly to the samples with axial alignment; they become dark at $\alpha = 0°$ and $\alpha = 90°$, and bright at 45°. However, at $\alpha = 45°$ the transmittance considerably depends on ϕ oscillating with a period of 180° [Fig. 6(a)]. This implies that the induced structures are not axially symmetrical. Further inspection of the dyed samples in polarized light showed that LC molecules are aligned perpendicularly to the light polarization. Besides, non-axiality of the induced alignment was confirmed by ϕ-rotations;

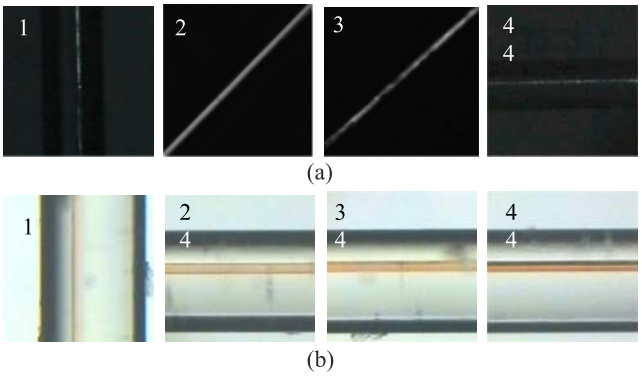

Fig. 6. Microphotographs of the capillary samples with transversal LC alignment configuration [Fig. 5(b)]: (a) sample filled with LC 6CHBT viewed between two of crossed polarizers having, accordingly, vertical and horizontal polarization axis: $\alpha = 0°$ (1), $\alpha = 45°$, $\phi = 90°$ (2), $\alpha = 45°$, $\phi = 0°$ (3), $\alpha = 90°$ (4); (b) sample filled with LC E7 doped by DR1 dichroic dye viewed in polarized light (vertical direction of polarization): $\alpha = 0°$ (1), $\alpha = 90°$, $\phi = 0°$ (2), $\alpha = 90°$, $\phi = 45°$ (3), $\alpha = 90°$, $\phi = 90°$ (4).

the samples demonstrated transmittance oscillations with a period of 180° [Fig. 6(b)]. Taking into account these results as well as planar anchoring at the capillary wall one can deduce that the transversal configuration presented in Fig. 5(b) is realized. It is formed in result of balance of anchoring and elastic forces and to some extend is similar to the bipolar structure of LC drops in polymer dispersed liquid crystals [30]. LC alignment in the direction perpendicular to light polarization is in a full agreement with the aligning properties of the photoalignment materials used.

3.1.3. Tilted alignment

Even more complicated configuration is obtained for $\varphi = 45°$. In crossed polarizers, these capillaries are bright at $\alpha = 0°$ and $\alpha = 90°$ (capillary axis parallel and perpendicular to polarizer axis, respectively) and dark at $\alpha = \pm 45°$ [Fig. 7(a)] implying that majority of LC molecules are in slanting position forming angle with the capillary axis about 45°. This is confirmed by observation of the probes filled by dyed LC in polarized light; these probes show minimal transmittance at $\alpha = 45°$ and maximal transmittance at $\alpha = -45°$ [Fig. 7(b)]. These probes also demonstrate very clear transmittance oscillation with a period 360° at rotation round their axis, if they are fixed in the position $\alpha = \pm 45°$. Note that this oscillation period is twice bigger than in a case of sample with transversal alignment. The major reason of this oscillation is the change of angle between the direction of light polarization and the alignment direction circumscribing the cone during sample rotation around its axis [see Fig. 7(c)]. It may be assumed that in the capillary sections tilted in 45° to the capillary axis, the alignment has bipolar structure similarly to the transversal configuration earlier discussed. This structure, coined as the tilted one, is presented in Fig. 5(c).

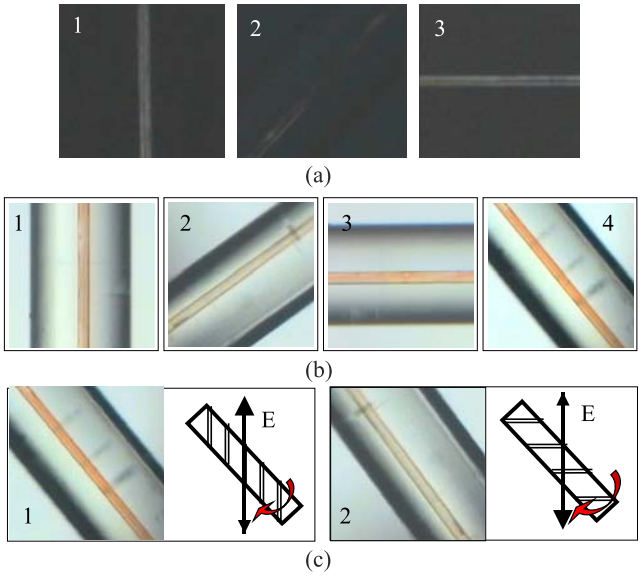

Fig. 7. Microphotographs of the capillary sample filled with the dyed LC E7 forming tilted alignment configuration [Fig. 5(c)]: (a) observation between two of crossed polarizers with, accordingly, vertical and horizontal polarization axis: $\alpha = 0°$ (1), $\alpha = 45°$ (2), $\alpha = 90°$ (3); (b, c) observation in vertically polarized light. Series (b) corresponds to α-rotation: $\alpha = 0°$ (1), $\alpha = 45°$ (2), $\alpha = 90°$ (3), $\alpha = 135°$ (4). Series (c) relates to ϕ-rotations: $\alpha = 135°$, $\phi = 180°$ (1), and $\alpha = 135°$, $\phi = 0°$ (2). The drawings in (c) schematically illustrate that the transmittance of the sample reaches its max and min if the induced alignment direction is, correspondingly, parallel and perpendicular to the direction of light polarization.

3.2. Alignment configurations in capillaries with homeotropic anchoring

The pictures corresponding to such a sample are presented in Fig. 8. One can, first of all, see that samples are nonuniform in the transversal direction meaning that the LC alignment in the core part of the capillary is different from that in the periphery part. According to the presented pictures, LC aligns homeotropically near the capillary wall and along the capillary axis in the central area. The brightness of this sample does not change during rotation around the capillary axis implying axial symmetry of the obtained configuration. This configuration is schematically presented in Fig. 5(d). This, so named, escaped radial (or splay) configuration was predicted in the early 1970s for the cylinder tubes with diameters larger than 0.1 μm and initially detected in the sub-micrometer-size nucleopore membranes [31]. The central area with the non-radial LC alignment is caused by the line disclination "escaped" along the axis of a cylindrical tube.

Finally, note that all alignment configurations described above were realized in capillaries of all diameters from the range 8–25 μm. In other words, in this range, the capillary size does not influence considerably alignment configuration of LC.

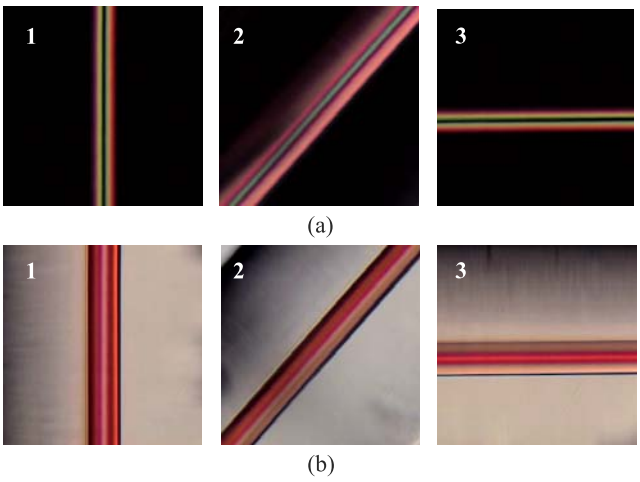

Fig. 8. Microphotographs of the capillary sample filled with the dyed LC E7 forming escaped radial alignment configuration [Fig. 5(d)]: (a) observation between two of crossed polarizers with, accordingly, vertical and horizontal polarization axis: $\alpha = 0°$ (1), $\alpha = 45°$ (2), $\alpha = 90°$ (3); and (b) observation in vertically polarized light: $\alpha = 0°$ (1), $\alpha = 45°$ (2), $\alpha = 90°$ (3).

4. Conclusions

In summary, by setting planar and homeotropic boundary conditions a variety of LC orientational configurations was realized in cylindrical microcapillaries with different diameters. In case of homeotropic anchoring, escaped radial configuration is realized with radial (homeotropic) and parallel alignment in the periphery and central part, respectively [Fig. 5(d)]. In the capillaries with planar anchoring, the alignment configuration was controlled by photoalignment technique. Depending on the polarization direction of the light, planar, transversal and tilted alignment structures were realized [Figs. 5(a–c)]. We predict that the number of LC structures obtainable by the photoalignment technique is much broader and our further attempts will be aimed at their realization. The approach developed in this study can be further applied to control LC alignment in photonic liquid crystal fibers showing big promise for various modern photonic applications.

Acknowledgements

This work was supported by the Polish Ministry of Science and Education under grants N517 056535 and N507 439539 and, partially, by the "Master" Program of the Polish Science Foundation. Authors thank I. Gerus, V. Syromyatnikov, V. Zagnii, L. Vretik, and L. Olkhovyk for providing photoaligning polymers.

References

1. P.S.J. Russell, "Photonic crystal fibers", *Science* **299**, 358–362 (2003).
2. J.C. Knight, "Photonic crystal fibers", *Nature* **424**, 847–851 (2003).
3. R. Buczyński, "Photonic crystal fibers", *Acta Phys. Pol.* **A106**, 141–168 (2004).
4. P.S.J. Russell, "Photonic-crystal fibers", *J. Lightwave Technol.* **24**, 4729–4749 (2006).
5. T.R. Woliński and A.W. Domański, "Polarization mode. Dispersion in birefringent optical fibers", *Acta Phys. Pol.* **A103**, 211–220 (2003).
6. T. Larsen, A. Bjarklev, D. Hermann, and J. Broeng, "Optical devices based on liquid crystal photonic bandgap fibres", *Opt. Express* **11**, 2589–2596 (2003).
7. F. Du, Y. Lu, and S.T. Wu, "Electrically tunable liquid-crystal photonic crystal fibers", *Appl. Phys. Lett*. **85**, 2181–2183 (2004).
8. J. Sun. and C.C. Chan, "Hybrid guiding in liquid-crystal photonic crystal fibers", *J. Opt. Soc. Am.* **B24**, 2640–2646 (2007).
9. T.R. Woliński, S. Ertman, P. Lesiak, A.W. Domański, A. Czapla, R. Dąbrowski, E. Nowinowski-Kruszelnicki, and J. Wójcik, "Photonic liquid crystal fibers – a new challenge for fiber optics and liquid crystals photonics", *Opto-Electron. Rev*. **14**, 329–334 (2006).
10. T. Woliński, A. Czapla, S. Ertman, M. Tefelska, A. Domański, J. Wójcik, E. Nowinowski-Kruszelnicki, and R. Dąbrowski, "Photonic liquid crystal fibers for sensing applications", *IEEE T. Instrum. Meas*. **57**, 1796–1802 (2008).
11. T. Nasiłowski, P. Lesiak, R. Kotyński, M.K. Antkowiak, F. Berghmans, P. Mergo, J. Wójcik, and H. Thienpont, "Multi--parameter sensitivities of birefringent photonic crystal fiber", *Proc. SPIE* **5576**, 68–73 (2004).
12. T.R. Woliński, S. Ertman, M. Tefelska, A. Czapla, D. Budaszewski, A.W. Domański, R. Dąbrowski, E. Nowinowski--Kruszelnicki, and J. Wójcik, "Polarizing and depolarizing optical effects in photonic liquid crystal fibers", *Mol. Cryst. Liq. Cryst*. **489**, 169–182 (2008).
13. K. Takatoh, M. Hasegawa, M. Koden, N. Itoh, R. Hasegawa, and M. Sakamoto, *Alignment Technologies and Applications of Liquid Crystal Devices*, Taylor & Frances, 2005.
14. K. Ichimura, Y. Suzuki, T. Seki, A. Hosoki, and K. Aoki, "Reversible change in alignment mode of nematic liquid crystal regulated photochemically by "command surfaces" modified with an azobenzene monolayer", *Langmuir* **4**, 1214–1216 (1988).
15. W.M. Gibbons, P.J. Shannon, S.T. Sun, and B.J. Swetlin, "Surface-mediated alignment of nematic liquid crystals with polarized laser light", *Nature* **351**, 49–50 (1991).
16. A. Dyadyusha, V. Kozinkov, T. Marusii, Y. Reznikov, V. Reshetnyak, and A. Khizhnyak, "Light-induced planar alignment of nematic liquid crystal on anisotropic surface without microgrooves", *Ukr. Fiz. Zh.* **36**, 1059–1061 (1991).
17. M. Schadt, K. Schmitt, V. Kozinkov, and V. Chigrinov, "Surface-induced parallel alignment of liquid crystals by linearly polymerized photopolymers", *Jpn. J. Appl. Phys.,* **31**, 2155–2164 (1992).
18. M. O'Neill and S.M. Kelly, "Photoinduced surface alignment for liquid crystal displays", *J. Phys. D: Appl. Phys*. **33**, R67–R84 (2000).
19. V. Chigrinov, *Photoalignment of Liquid Crystal Materials: Physics and Application,* Wiley-SID series, UK, 2008.

20. V. Presnyakov, Z. Liu, and V. Chigrinov, "Infiltration of photonic crystal fiber with liquid crystals", *Proc. SPIE* **6017**, 60170J-1 (2005).
21. S. Ertman, T.R. Woliński, A. Czapla, K. Nowecka, E. Nowinowski-Kruszelnicki, and J. Wójcik, "Liquid crystal molecular orientation in photonic liquid crystal fibers with photopolymer layers", *Proc. SPIE* **6587**, 658706-7 (2007).
22. M.S. Chychłowski, S. Ertman, and T.R. Woliński, "Analysis of liquid crystals orientation in microcapillaries", *Photonics Letters of Poland* **2**, 28–33 (2010).
23. M.S. Chychłowski and T.R. Woliński, "Splay orientation in a capillary", *Photonics Letters of Poland* **2**, 180–182 (2010).
24. M.S. Chychłowski, S. Ertman, M.M. Tefelska, T.R. Woliński, E. Nowinowski-Kruszelnicki, and O. Yaroshchuk, "Photo-induced orientation of nematic liquid crystals in microcapillaries", *Acta Phys. Pol.* **A118**, 1100–1103 (2010).
25. S.B. Kwon, K.J. Kim, Y.S. Choi, I. Gerus, A. Dyadyusha, and Y. Reznikov, United States Patent 6,399,165, filed Nov. 16, 1998.
26. V. Chigrinov, E. Prudnikova, V. Kozenkov, H. Kwok, H. Akiyama, T. Kawara, H. Takada, and H. Takatsu, "Synthesis and properties of azo dye aligning layers for liquid crystal cells", *Liq. Cryst.* **29**, 1321 (2002).
27. L. Vretik, V. Syromiatnikov, V. Zagniy, L. Paskal', O. Yaroshchuk, L. Dolgov, V. Kyrychenko, and C.D. Lee, "Polymethacryloylarylmethacrylates: New concept of photoalignment materials for liquid crystals", *Mol. Cryst. Liq. Cryst.* **479**, 121–134 (2007).
28. Y.J. Wang and G.O. Carlisle, "Optical properties of DR1 doped liquid crystals", *J. Mater. Sci.-Mater. El.* **13**, 173–178 (2002).
29. P.J. Collings, B.R. Ratna, and R. Shashidhar, "Order parameter measurements of dichroic dyes dissolved in smectic liquid crystals that tilt without layer contraction", *Phys. Rev.* **E67**, 021705 (2003).
30. P.S. Drzaic, *Liquid Crystal Dispersions* **1**, Series on Liquid Crystals, World Scientific, Singapore, 1995.
31. P. Crawford, M. Vilfan, J.W. Doane, and I. Vilfan, "Finite molecular anchoring in the escaped-radial nematic configuration: A^2NMR study", *Phys. Rev.* **A43**, 836 (1991).